

David O. Olawale · Okenwa O.I. Okoli  
Ross S. Fontenot · William A. Hollerman  
*Editors*

# Triboluminescence

Theory, Synthesis, and Application

 Springer

# Triboluminescence



David O. Olawale • Okenwa O.I. Okoli  
Ross S. Fontenot • William A. Hollerman  
Editors

# Triboluminescence

Theory, Synthesis, and Application

 Springer

*Editors*

David O. Olawale  
Industrial and Manufacturing  
Engineering Department  
FAMU-FSU College of Engineering  
Tallahassee, FL, USA

Okenwa O.I. Okoli  
Industrial and Manufacturing  
Engineering Department  
FAMU-FSU College of Engineering  
Tallahassee, FL, USA

Ross S. Fontenot  
Naval Surface Warfare Center  
Bethesda, MD, USA

William A. Hollerman  
Department of Physics  
University of Louisiana  
Lafayette, LA, USA

ISBN 978-3-319-38841-0

ISBN 978-3-319-38842-7 (eBook)

DOI 10.1007/978-3-319-38842-7

Library of Congress Control Number: 2016944358

© Springer International Publishing Switzerland 2016

This work is subject to copyright. All rights are reserved by the Publisher, whether the whole or part of the material is concerned, specifically the rights of translation, reprinting, reuse of illustrations, recitation, broadcasting, reproduction on microfilms or in any other physical way, and transmission or information storage and retrieval, electronic adaptation, computer software, or by similar or dissimilar methodology now known or hereafter developed.

The use of general descriptive names, registered names, trademarks, service marks, etc. in this publication does not imply, even in the absence of a specific statement, that such names are exempt from the relevant protective laws and regulations and therefore free for general use.

The publisher, the authors and the editors are safe to assume that the advice and information in this book are believed to be true and accurate at the date of publication. Neither the publisher nor the authors or the editors give a warranty, express or implied, with respect to the material contained herein or for any errors or omissions that may have been made.

Printed on acid-free paper

This Springer imprint is published by Springer Nature

The registered company is Springer International Publishing AG Switzerland

# Preface

The triboluminescence phenomenon, since its first recorded discovery in 1605, has enjoyed extensive studies targeted at understanding the underlying mechanism, discovery, and synthesis of new materials, their characterization, and applications in civil and aerospace engineering systems. Significant progress has been made in these areas since the last text that was written over 35 years ago. The need to concisely document the significant progress that has been made in this field in the last 35 years necessitated this book.

The book expounds on progress made over the last 35 years in the theory, synthesis, and application of triboluminescence for creating smart structures. It presents in detail research into the utilization of the triboluminescent properties of certain crystals as new sensor systems for smart engineering structures. These triboluminescence-based sensor systems have the potential to enable wireless, in situ, real-time and distributed (WIRD) damage, stress, and impact sensing in civil and aerospace systems like bridges, aircrafts, space crafts, and wind blades.

Furthermore, the book is divided into three sections according to the covered areas which are the theory, synthesis, and application of the triboluminescence phenomenon. In order to ensure depth and breadth in the coverage of these key areas, the editors worked with leading experts in the field from all over the world to author the very insightful chapters in the book. The book is written to present information on triboluminescence relevant to engineers and scientists across a range of fields, including aerospace, defense, civil infrastructure, and wind energy. The goal is to facilitate readers' understanding with concise treatments of the topics covered in the text.

In conclusion, we would like to express our profound gratitude to all our contributing authors for the great depth and expertise they have brought to this book. You have helped in documenting the various advances made in the field for the benefits of the present and coming generations. Thanks for all the hard work and

timely submission of the manuscripts. We are particularly grateful to our publishing team at Springer. Special thanks to Michael Luby and Ms. Brinda Megasyamalan for their support, patience, and guidance throughout the project.

Tallahassee, FL  
Tallahassee, FL  
Bethesda, MD  
Lafayette, LA  
March, 2016

David O. Olawale  
Okenwa O.I. Okoli  
Ross S. Fontenot  
William A. Hollerman

# Contents

<b>1 Introduction to Triboluminescence . . . . .</b>	<b>1</b>
David O. Olawale, Ross S. Fontenot, Md Abu S. Shohag, and Okenwa O.I. Okoli	
<b>2 Nature of the Electronic Charge Carriers Involved in Triboluminescence . . . . .</b>	<b>17</b>
Friedemann T. Freund	
<b>3 Mechanoluminescence of Coordination Compounds . . . . .</b>	<b>39</b>
Ercules Epaminondas Sousa Teotonio, Wagner Mendonça Faustino, Hermi Felinto Brito, Maria Claudia França Cunha Felinto, Jandeilson Lima Moura, Israel Ferreira Costa, and Paulo Roberto Silva Santos	
<b>4 Luminescence of Triboplasma: Origin, Features, and Behavior . . . . .</b>	<b>65</b>
Roman Nevshupa and Ken'ichi Hiratsuka	
<b>5 Triboluminescence of Liquid Dielectrics: On a Way to Discover the Nature of Sonoluminescence . . . . .</b>	<b>95</b>
D.A. Biryukov and D.N. Gerasimov	
<b>6 Functional Triboluminescent Nanophase for Use in Advanced Structural Materials: A Smart Premise with Molecular and Electronic Definition . . . . .</b>	<b>125</b>
M. Jasim Uddin, David O. Olawale, Jin Yan, Justin Moore, and Okenwa O.I. Okoli	
<b>7 Europium Tetrakis Dibenzoylmethide Triethylammonium: Synthesis, Additives, and Applications . . . . .</b>	<b>147</b>
Ross S. Fontenot, Kamala N. Bhat, William A. Hollerman, and Mohan D. Aggarwal	

**8 Mechanoluminescence Induced by Acoustic Cavitation . . . . . 237**  
Nathan C. Eddingsaas

**9 Triboluminescence of Inorganic Lanthanide Salts . . . . . 273**  
G.L. Sharipov and A.A. Tukhbatullin

**10 Triboluminescent Sensors for Polymer-Based Composites . . . . . 305**  
Kunal Joshi, Margaret Scheiner, David O. Olawale,  
and Tarik J. Dickens

**11 Detection of Low-Velocity-Impact Triboluminescent  
Emissions . . . . . 333**  
Shawn M. Goedeke, William A. Hollerman,  
Stephen W. Allison, and Ross S. Fontenot

**12 3D Sensing Using Solid-State Wire-Shaped Photovoltaic  
Sensor in TL-Based Structural Health Monitoring . . . . . 351**  
Jin Yan, M. Jasim Uddin, David O. Olawale, Tarik J. Dickens,  
and Okenwa O.I. Okoli

**13 Triboluminescent Sensors for Cement-Based Composites . . . . . 379**  
David O. Olawale, Jasim M. Uddin, Jin Yan, Tarik J. Dickens,  
and Okenwa O.I. Okoli

**14 Triboluminescence at Speeds Greater than 100 m/s . . . . . 411**  
Ross S. Fontenot, William A. Hollerman,  
and Noah P. Bergeron

**Index . . . . . 445**

# Chapter 1

## Introduction to Triboluminescence

David O. Olawale, Ross S. Fontenot, Md Abu S. Shohag,  
and Okenwa O.I. Okoli

### 1.1 Luminescence

Light emission in a material can either be by incandescence or luminescence. Figure 1.1 gives an overview of some the various forms by which light can be produced [1]. Incandescence is light produced by heating an object to such a high temperature that the atoms become highly agitated leading to the glowing of the bulk matter [2]. It is an inefficient way of producing light as most of the energy is dissipated as heat. Incandescence is explained by Planck's black body emission theory. On the other hand, luminescence, sometimes referred to as "cold light," is light produced at normal and lower temperatures [3]. It involves an energy source elevating an electron of an atom out of its "ground" state into an "excited" state; and the sequential release of energy in the form of light when the electron returns to its ground state [2]. It is a more efficient mechanism of light emission.

Wiedemann identified six kinds of luminescences based on the method of excitation [4]. These are photoluminescence, thermoluminescence, electroluminescence, crystalloluminescence, triboluminescence, and chemiluminescence (Fig. 1.1). Photoluminescence of solids is excitation by light and is subdivided

---

D.O. Olawale (✉)

Nanotechnology Patronas Group Inc., 914 Railroad Ave., Tallahassee, FL 32310, USA

Department of Industrial and Manufacturing Engineering, FAMU-FSU College  
of Engineering, 2525 Pottsdamer Str., Tallahassee, FL 32310, USA

e-mail: [doo07@my.fsu.edu](mailto:doo07@my.fsu.edu)

R.S. Fontenot

Carderock Division, Naval Surface Warfare Center, Code 6301, West Bethesda,  
MD 20817, USA

M.A.S. Shohag • O.O.I. Okoli

Department of Industrial and Manufacturing Engineering, FAMU-FSU College  
of Engineering, 2525 Pottsdamer Str., Tallahassee, FL 32310, USA

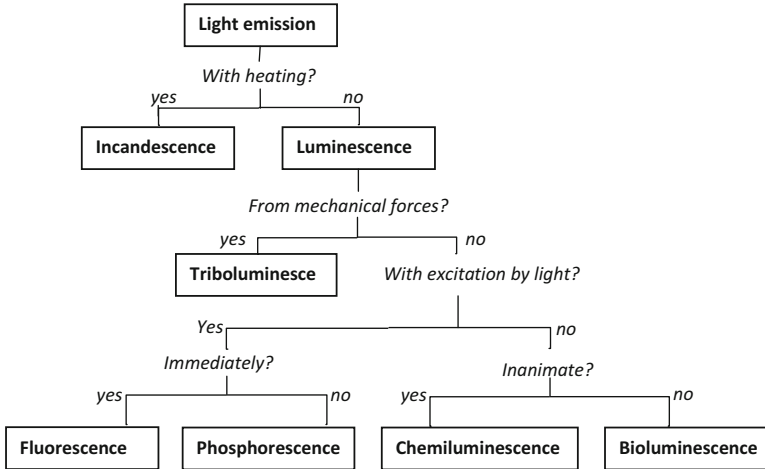


**Fig. 1.1** Overview of different light emission mechanisms [1]

into fluorescence and phosphorescence. Thermoluminescence is light produced from excitation by gentle heating. Electroluminescence is caused by excitation of gases in electrical fields. Crystalloluminescence is from excitation resulting from solution crystallization while triboluminescence is from excitation of crystals when they are stressed or broken. Chemiluminescence occurs during chemical reaction and all bioluminescence, occurring in living organisms, are examples of chemiluminescence [4].

Light-induced luminescence can be classified based on the time delay between the completion of the excitation process and the start of photon emission for a luminescent material [5]. Fluorescence is luminescence that occurs when photons emission is due to a direct transition of less than 10 ms decay time. It is the process where light emission is ruled by the lifetime of the emitting center. Materials that emit fluorescence are known as fluors and are used for applications where timing is important. Increasing the temperature of a substance generally reduces its fluorescence. Phosphorescence is luminescence that persists for more than 100 ms after cessation of irradiation [5]. Phosphorescent materials can emit luminescence many hours after cessation of excitation. During phosphorescence, atomic transitions through intermediate metastable states determine the exact duration of the phosphorescence. Materials that emit phosphorescence are known as phosphors and are used in powdered form for lamps, television screens, and related purposes. However, the light from phosphors in these applications exhibit decay times less than 10 ms [5]. The remaining part of this chapter focuses on triboluminescence.

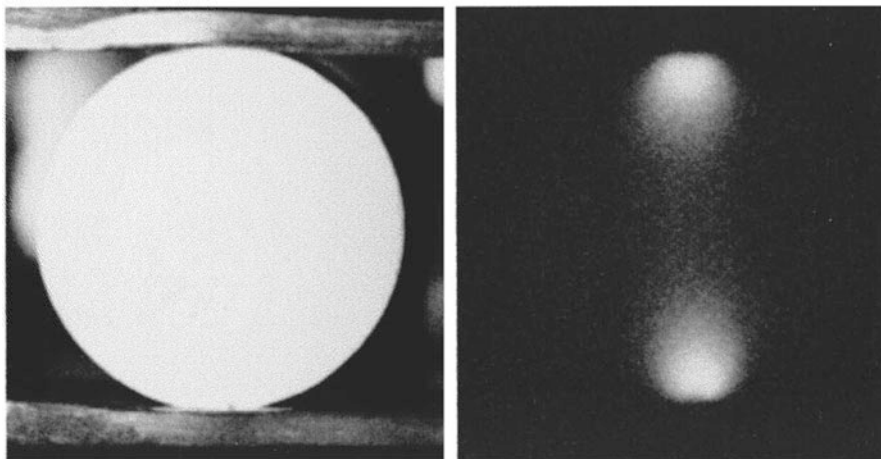


**Fig. 1.2** Stressed SrAl<sub>2</sub>O<sub>4</sub>:Eu and the triboluminescence image under a compressive load of 1000 N [21]

## 1.2 Triboluminescence

Triboluminescence, also known as fracto- [6], piezo- [7], mechano- [8], crystallo-, or sono-luminescence [9, 10], is the emission of light by solid materials when they are stressed or fractured [3, 11, 12]. The term triboluminescence was coined by Wiedemann in 1888 [13] and it basically means light from friction, as the term comes from the Greek word *tribein*, meaning “to rub,” and the Latin prefix *lumin*, meaning “light” [5]. Triboluminescence has been observed in various luminescent processes such as [9] emission during breaking of adhesive bonds [14, 15]; shaking of mercury in a glass vessel [16]; rapid crystallization of certain substances [17]; collapse of small gas bubbles in a liquid [18]; excitation of a laser-induced shock wave in solids [19]; elastic and plastic deformation of solids; scratching; milling; and fracture [13, 20]. The phenomenon was first studied by Sir Francis Bacon with sugar as recorded in *The Advancement of Learning* in 1605 [5, 13]. Figure 1.2 shows the stressed SrAl<sub>2</sub>O<sub>4</sub>:Eu sample and the TL image under a compressive load of 1000 N. The stressed sample emitted intense visible green light from its two ends.

Although triboluminescence phenomenon has been studied for centuries, it remains an enigma at the conceptual and theoretical levels [9]. The phenomenon is closely related to both friction and wear and all three require an understanding of the highly nonequilibrium processes occurring at the molecular level [22]. These processes are significantly different depending on the tribological conditions, environment and materials [9]. The emission spectrum for sugar indicates that the light comes from the atmospheric nitrogen that fills the gap during fracture; the same source of light as lightning or touching a doorknob on a winter day. On the other hand, spectra for other samples show emission from the material as well as

the nitrogen lines, suggesting a secondary energy process. Furthermore, other materials show a spectrum characteristic of the material without the nitrogen lines. While the abrupt charge separation is the same in all cases, the mechanism (s) of emission depend on the material [5].

### 1.3 Elastico-, Plastico-, and Fracto-Triboluminescence

Triboluminescence may be divided in to three types: namely (1) elástico-, (2) plástico- and (3) fracto-triboluminescence [3, 23].

#### 1.3.1 *Elastico-Triboluminescence*

Elastico-triboluminescence is luminescence produced during the elastic deformation of solids, where neither fracture nor plastic deformation is required [3]. This can be by mechanical or electrostatic interaction of dislocations with defect centers, or by thermal excitation in the stressed regions of crystals that exhibit elástico-triboluminescence such as x- or  $\gamma$ -irradiated alkali halides and ZnS:Mn [23].

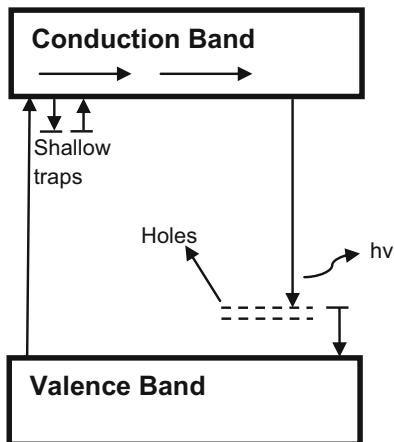
Chandra et al. [24] provided experimental evidence supporting the suitability of a piezoelectrically stimulated electron detrapping model as being responsible for the elastic and plastic triboluminescence of ZnS:Mn. The suggested steps for elástico-triboluminescence in ZnS:Mn based on the piezoelectric mechanism [24] are as follows: The deformation of ZnS:Mn crystals produces piezoelectric field because the crystal structure of ZnS is non-centrosymmetric [25]. The piezoelectric field results in decrease in the trap-depth which causes detrapping of electrons from filled-electron traps, with the electrons reaching the conduction band as illustrated in Fig. 1.3. The electrons may recombine with the holes trapped in the defect centers or they may fall to the valence band with the energy being released non-radiatively. The energy released non-radiatively may be transferred to the  $Mn^{2+}$  ions to cause their excitation [26–29]. The de-excitation of excited  $Mn^{2+}$  ions gives rise to the light emission characteristic of the  $Mn^{2+}$  ions.

Elastico-triboluminescence in ZnS:Mn starts at a pressure of about 1 MPa ( $10^6 \text{ Nm}^{-2}$ ) [30]. The piezoelectric charge density  $\gamma$  generated at this pressure in the crystal with a piezoelectric constant ( $d_{33} = 3.3 \times 10^{-11} \text{ CN}^{-1}$ ) [31] will be  $3.3 \times 10^{-5} \text{ Cm}^{-2}$ . This will result in an electric field  $F$  given by the relation

$$F = \gamma/\epsilon_0 \quad (1.1)$$

The permittivity  $\epsilon_0$  of the crystal is  $8.85 \times 10^{-12} \text{ CNm}^{-2}$ ; consequently, an electric field of about  $3.7 \times 10^6 \text{ Vm}^{-1}$  or  $3.7 \times 10^4 \text{ V cm}^{-1}$  will be developed near the crystal surface [30]. The internal electric field will however be about one order less than the external field on the crystal surface because the dielectric

**Fig. 1.3** Schematic of elasto-triboluminescence in ZnS:Mn [3]



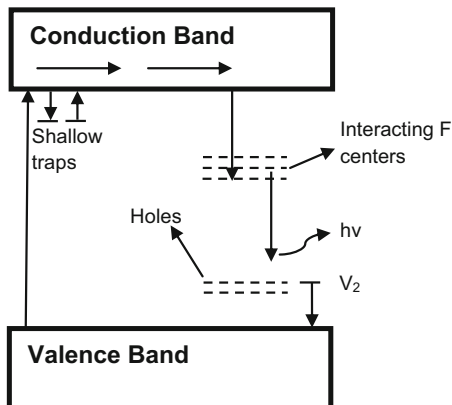
constant of ZnS crystals is 8.8 [30]. An electric field of the order of  $10^6 \text{ V cm}^{-1}$  is however needed to cause electron detrapping from traps or the impact excitation of  $\text{Mn}^{2+}$  centers [30]. The local electric field near  $\text{Mn}^{2+}$  ions may however be higher because of the local change in the crystals' structure near  $\text{Mn}^{2+}$  sites [32, 33]. This may result in a higher piezoelectric constant near the  $\text{Mn}^{2+}$  sites [34, 35] to generate an electric field of the order of  $10^5 \text{ V cm}^{-1}$  that may cause sufficient decrease in the trap-depth but not sufficient to cause the impact excitation of  $\text{Mn}^{2+}$  centers [30]. Subsequent electron-hole recombination may release energy non-radiatively for the excitation of  $\text{Mn}^{2+}$  centers.

### 1.3.2 *Plastico-Triboluminescence*

Plastico-triboluminescence is luminescence produced during plastic deformation of solids where fracture is not required. It can be excited by the mechanical or electrostatic interaction of dislocations with defect centers; electrification of crystal surfaces by the movement of charged dislocations; or thermal excitation in the stressed regions of solids like colored alkali halides, II–VI compounds, alkaline-earth oxides, and metals [23]. Chandra et al. [36] reported on the luminescence arising from the plastic deformation of colored alkali halides using pressure steps. In the elastic region, the strain increases linearly with the stress, and the triboluminescent intensity also increased linearly with stress. In the plastic region, the strain and TL intensity increased with stress according to the power law [36].

The suggested steps involved in the TL of x- or  $\gamma$ -irradiated alkali halide crystals are as illustrated in Fig. 1.4: (1) Plastic deformation causes movement of dislocations. (2) The moving dislocations capture electrons from the interacting F-centers lying in the expansion region of dislocations. (3) The captured electrons from F-centers move with the dislocations and they also drift along the axes of

**Fig. 1.4** Energy level diagram of mechanoluminescence of colored alkali halide crystals [37]



dislocations. (4) The recombination of dislocation-captured electrons with the holes lying in the dislocation donor band gives rise to the light-emission characteristic of the halide ions in hole centers [38].

The triboluminescent (TL) intensity  $I$  was found to be directly related to  $\eta$ , the efficiency of radiative electron–hole combination, and  $n_d$ , the number of electrons in the dislocation band at any time  $t$  as follows:

$$I = \eta\beta n_d = \frac{\eta P_0^m m \xi p_f r_f n_f}{K^m b \lambda (\xi - \phi)} [\exp(-\phi t) - \exp(-\xi t)] \quad (1.2)$$

where  $\beta = 1/\tau_d$ ,  $\tau_d$  is the lifetime of electrons in the dislocations band,  $P_0$  is the final value of pressure,  $\xi = 1/t_r$ ,  $t_r$  is the time constant for rise of pressure,  $K$  is referred to as the strength coefficient,  $n$  is the work-hardening exponent,  $m = 1/n$ ,  $p_f$  is the probability of capture of interacting F-center electrons by the dislocations,  $r_f$  is the radius of interaction between the moving dislocations and F-centers,  $n_f$  is the density of F-centers in the crystals,  $\phi = 1/\tau_p$ ,  $\tau_p$  is the pinning time of the dislocations,  $b$  is the Burgers vector, and  $\lambda$  is the mean free path of the moving dislocations. The maximum triboluminescent intensity  $I_m$  is given as

$$I_m = \frac{P_0^m m \xi p_f r_f n_f}{K^m b \lambda} \quad (1.3)$$

The total intensity is given as

$$I_t = \int_0^\infty I dt = \frac{P_0^m m \xi p_f r_f n_f}{K^m b \lambda \phi} \quad (1.4)$$

The  $I_m$  and  $t_m$  increase according to the power law with an increase in the applied pressure. It has also been shown that the TL intensity depends on many parameters

including strain rate, stress, density of F-centres, size of crystals, temperature, and luminescence efficiency [13, 23, 39, 40]. The following relationships show the effect of temperature on the triboluminescent response [36]:

$$I_m = \frac{P_0^m m \xi p_{f0} r_f n_f}{K^m b \lambda} \exp(-E_a/KT) \quad (1.5)$$

The total intensity is given as

$$I_t = \int_0^{\infty} I dt = \frac{P_0^m m \xi p_{f0} r_f n_f}{K^m b \lambda \phi} \exp(-E_a/KT) \quad (1.6)$$

where  $E_a$  is the energy gap between the bottom of the dislocation band and the average ground state of the interacting F-centers. The  $I_m$  and  $I_t$  increase with increase in temperature because at low temperature,  $\exp(-E_a/KT)$  increases with temperature. However, at higher temperature,  $I_m$  and  $I_t$  decrease because  $n_f$  decreases as a result of thermal quenching. Hence,  $I_m$  and  $I_t$  are optimum for a particular temperature of the crystals.

### 1.3.3 Fracto-Triboluminescence

Fracto-triboluminescence is luminescence produced due to the creation of new surfaces during the fracture of solids. During fracto-triboluminescence, there is creation of charged surfaces at fracture (Fig. 1.5) due to processes such as piezoelectrification, movements of charged dislocations, and charged defect barodiffusion [23, 41]. There is neutralization of these surface charges by the charge carriers or ions produced from the dielectric breakdown of the intervening gases and solids. This results in the production of luminescence that resembles a gas discharge (e.g., sucrose, tartaric acid, Rochelle salt) or luminescence of a solid (e.g., coumarin, resorcinol, and phenanthrene) or one that combines the characteristics of both the intervening gases and solids (e.g., uranyl nitrate hexahydrate, impure saccharin, and chlorotriphenyl-methane [12, 23]).

If a crystal with thickness  $H$  is cleaved along a plane parallel to its width  $W$ , with velocity of crack propagation being  $v$ , provided  $\alpha_3 t < 1$ , then the TL intensity may be given as [23]

$$I = 2(\eta_1 \alpha_1 + \eta_2 \alpha_2) \gamma w v t \quad (1.7)$$

where  $\gamma$  is the charge density of the newly created surfaces,  $\alpha_1$  and  $\alpha_2$  are the rate constants for the relaxation of charges on the newly created surfaces,  $\alpha_3 = \alpha_1 + \alpha_2$ , and  $\eta_1$  is the luminescence efficiency associated with the movement of carriers produced by the dielectric breakdown of the crystals while  $\eta_2$  is the efficiency

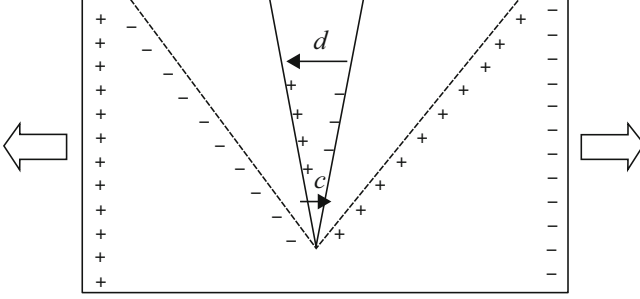


**Fig. 1.5** A schematic of the piezoelectric theory illustrating TL phenomena upon cleavage [41]

associated with the movement of electrons and ions produced by the dielectric breakdown of intervening gases. According to Eq. (1.7), when a crystal is cleaved, the TL intensity should rise linearly with time  $t$ . At the end of cleavage (at  $t = t_m$ ,  $v = 0$ ), the TL intensity may be expressed as

$$I = [\eta_1 \alpha_1 + \eta_2 \alpha_2] Q_0 \exp[-\alpha_3(t - t_m)] \quad (1.8)$$

where  $Q_0$  is the surface charge at  $t = t_m$ .

Equation (1.8) shows the exponential decay of the TL intensity after the cleavage of the crystals.

Triboluminescence can be used to determine the velocity of crack propagation in crystals [23] as follows:

$$v = H/t_m \quad (1.9)$$

The peak TL intensity at  $t = t_m$  is given as

$$I_m = (\eta_1 \alpha_1 + \eta_2 \alpha_2) \gamma A \quad (1.10)$$

where  $A = 2WH$  is the area of the newly created surfaces. Equation (1.10) implies that  $I_m$  should increase linearly with  $A$  and  $\gamma$ . The total intensity  $I_T$  is given as

$$I_T = \int I dt = (\eta_1 \alpha_1 + \eta_2 \alpha_2) \gamma A / \alpha_3 \quad (1.11)$$

When  $\alpha_2 = 0$ , that is no gaseous discharge as is the case with ZnS:Mn, the emission will be primarily bulk triboluminescence and  $\alpha_3 = \alpha_1$ . When  $\alpha_2 = 0$ , that is, no bulk triboluminescence—emission is primarily by gaseous discharge, and  $\alpha_3 = \alpha_2$ . Based on Eqs. (1.10) and (1.11),  $I_m$  and  $I_T$  should decrease with increase in temperature because  $\eta_1$ ,  $\eta_2$ , and  $\gamma$  decrease with temperature increase. However, a specific temperature may be reached above which  $\gamma$  may decrease to the point that the breakdown of gases and solids becomes impossible, and triboluminescence no longer occurs [23].

## 1.4 Triboluminescent Materials

According to Virk [4], the year 1603 was the beginning of modern luminescent materials because the first artificial phosphor described in Western literature dates from this year. In an effort to create gold, the Italian shoemaker and alchemist, Vincenzo Cascariolo, heated the natural mineral barite ( $\text{BaSO}_4$ ) to create a persistent luminescent material called Bolognian stone. The host material was BaS making it the first sulfide phosphor ever synthesized [11] and the first scientifically documented material to show persistent luminescence [4]. In the same vein, Francis Bacon in 1605 made the first recorded observation of triboluminescence in his writings, “Advancement of Learning,” about sparkling light from hard sugar when scrapped with a knife [41]. In 1684, Waller reported that when substances such as white sugar, loaf sugar, and rock salt were crushed in a mortar, they gave such intense light that the sides of the mortar and shape of the pestle could distinctly be displayed [23]. Friedrich Hoffmann synthesized CaS as a phosphor in 1700 while J. F. John synthesized SrS in 1817 [4]. The luminescent properties of ZnS, one of the most important luminescent hosts in the twentieth century, were not recognized until 1866, when the Sidot blend (hexagonal ZnS) was developed by Theodor Sidot in France [8].

The main contribution of early nineteenth-century research was the compilation of an extensive list of TL materials using highly subjective visual observation of the TL response as a function of time and quantity [13]. The development of the photomultiplier tube (PMT) in the 1930s and its application in triboluminescence studies in 1952 introduced a quantitative technique for detecting, measuring, and comparing TL emissions objectively.

The discovery of phosphor-based high-field electroluminescence in solids in 1936 is credited to Destriau [42]. Between late nineteenth and early twentieth centuries, Philip E.A. Lenard and his colleagues used different rare earth ions in addition to heavy metal ions as luminescent ions in different host materials to create new phosphors [43]. Hurt et al. synthesized europium dibenzoylmethide triethylammonium ( $\text{EuD}_4\text{TEA}$ ), also known as europium tetrakis, in 1966 [44].  $\text{EuD}_4\text{TEA}$  is an organic material in which triboluminescence can be observed in daylight [44, 45]. It has been estimated that 30 % of organic crystals and 50 % of inorganic crystals are triboluminescent [13].

Triboluminescent (TL) materials are being used to develop sensor systems for engineering structures [46–49]. Triboluminescence-based sensor systems have the potential for wireless, in situ, real-time, and distributed (WIRD) sensing that can enable continuous monitoring of civil and aerospace structures [3]. Researchers have investigated the application of TL in damage detection [11, 48]. They can be used as stress, fracture, and damage sensors [24, 50]. They have also been proposed for visualizing the stress field near the crack-tip, stress distribution in solids, and quasi-dynamic crack-propagation in solids [47, 49–53].

Any candidate triboluminescent material for this purpose should however have a large triboluminescent emission yield, be readily available, be environmentally

**Table 1.1** Triboluminescence of various materials [49]

Group	Sample	TL intensity (cps) <sup>a</sup>
Hexagonal	ZnS	60
	ZnS–Mn <sub>0.05</sub>	2800
	ZnS–Cu <sub>0.01</sub>	1100
	Zn <sub>2</sub> SiO <sub>4</sub> :Mn <sub>0.01</sub>	57
	ZnO	3
	SiC	4
X <sub>2</sub> O <sub>3</sub> (X = Al or Y)	α-Al <sub>2</sub> O <sub>3</sub>	10
	α -Al <sub>2</sub> O <sub>3</sub> :Mn <sub>0.01</sub>	60
	Y <sub>2</sub> O <sub>3</sub>	9
	Y <sub>2</sub> O <sub>3</sub> :Eu	20
	MgAl <sub>2</sub> O <sub>4</sub>	31
	CaAl <sub>2</sub> O <sub>4</sub>	14
	SrAl <sub>2</sub> O <sub>4</sub>	36
Fluorite	ZrO <sub>2</sub>	8
	HfO <sub>2</sub>	3
	CeO <sub>2</sub>	3
Perovskite	YBa <sub>2</sub> Cu <sub>4</sub> O <sub>8</sub>	1
	PbZr <sub>0.52</sub> Ti <sub>0.48</sub> O <sub>3</sub>	3
	Pb <sub>0.93</sub> La <sub>0.07</sub> Zr <sub>0.60</sub> Ti <sub>0.40</sub> O <sub>3</sub>	3

<sup>a</sup>TL intensity was measured as a function of friction applied to the material by a brass rod of 1 mm diameter under a load of 5 N and slide speed of 6.3 cm/s (2.5 rps)

benign, and be compatible with the host material [3, 45]. Xu et al. [49] compared the triboluminescent performance of different inorganic materials under identical mechanical stress conditions and obtained similar results for thin film and bulk materials (Table 1.1). The ZnS-based materials showed much higher TL intensities while the ZnS doped with Mn exhibited the highest luminous intensity of all the materials tested (Fig. 1.6a). It was shown that a manganese doping level of about 5 % gives the highest TL response (Fig. 1.6b) making ZnS:Mn a strong candidate for TL-based sensor systems.

The hexagonal crystal structure of ZnS:Mn is considered “loose” because it emits light with very little stress applied [45] such as by simply scratching it with a nail or any sharp object. Materials such as ZnS:Mn are usually made up of a semiconductor host (ZnS) and an impurity (Mn) called the dopant. The dopant concentration is usually a small fraction of the composition but it plays the critical function of changing the band structure of the crystal, thereby narrowing the energy gap between conduction and valence bands. With narrower energy gaps, transitions that emit light are more probable and this increases the opportunity for light to be emitted during excitation or relaxation of electrons [45].

In a more recent study, Hollerman et al. [45] measured the relative triboluminescent emission yields for 27 candidate triboluminescent materials powders under impact loading using a low energy drop tower. The goal was to compare the

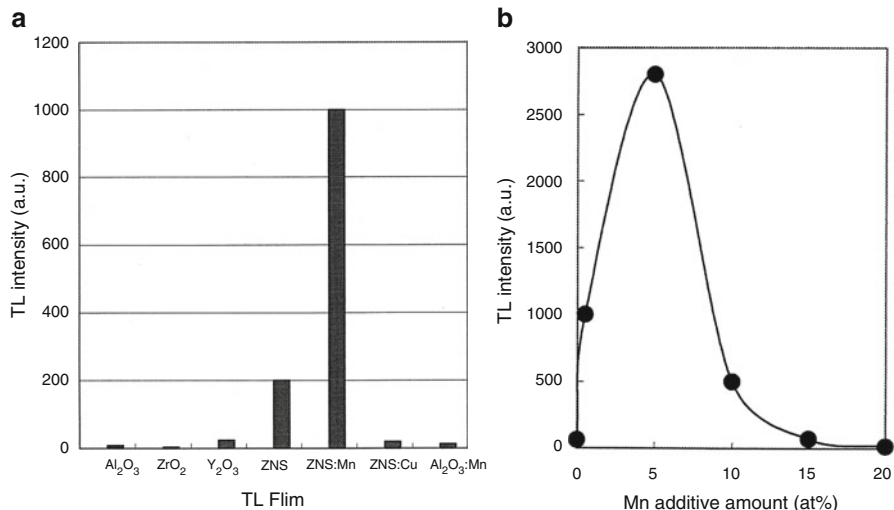


**Fig. 1.6** (a) TL intensity of various inorganic thin films under the same friction conditions and (b) effect of Mn additive amount on TL intensity [49]

triboluminescent emission yields for ZnS-based materials as a function of grain size and dopants (Table 1.2). The study included three organic Europium based luminescent materials (LM 9, 181, 194). The result shows that the EuD<sub>4</sub>TEA sample doped with dimethyl methylphosphonate (DMMP) (LM- 194) has the largest tested triboluminescent yield for all the tested materials [45]. It had over 3.19 times the triboluminescent yield compared to the baseline 7.5  $\mu\text{m}$  ZnS:Mn. In addition, the 19.8  $\mu\text{m}$  ZnS:Mn (LM-33) has the largest triboluminescent yield among all the tested inorganic materials. It was proposed that the method used to prepare LM-33 in terms of grain size, trap concentration, and dopant concentration, was responsible for the increased triboluminescent yield. The low yield from LM-88 and LM-89 ZnS:Mn may be accounted for by the 40% manganese in the formulation. On average, ZnS:Mn,Cu tends to have a larger triboluminescent yield compared to ZnS:Mn. No triboluminescence was observed with impact loading of the 5 nm sized ZnS:Mn powder. It is likely that the small 5 nm ZnS:Mn particles were trapped in surface imperfections and were not subject to sufficient force to produce triboluminescence [45]. Compared to ZnS:Mn, EuD<sub>4</sub>TEA appears to be more easily damaged than ZnS:Mn. The triboluminescent yield for EuD<sub>4</sub>TEA decreases by a factor of three from drops one to five whereas, the triboluminescent yield for ZnS:Mn only decreases by only about 10% for the same number of drops.

Finally, the compatibility of the TL material with the host matrix is vital to manufacturing and implementation of TL-based sensor systems [3] because the TL material cannot function as a sensor on its own. For integration into composite material systems, it might be necessary that the host matrix have a melting point greater than the cure temperature of the composite and also need to be chemically compatible with it [54]. Sage et al. [54] provided information about the melting

**Table 1.2** Comparison of the triboluminescent yields for the 27 luminescent materials (LM) as measured using the drop tower [45]

Base material	Sample mass (g)	LM number	Lot number	Manufacturer	Grain size ( $\mu\text{m}$ )	Yield ratio <sup>a</sup>
ZnS:Mn	1	171	1	Center for Integrated Nanotechnologies <sup>b</sup>	0.005	0.000
	1/0.1	34	15,248	Phosphor technology	7.5	1.000/1.000 <sup>a</sup>
	1	7	17,112	Phosphor technology	8.5	1.223
	1	117	19,252	Phosphor technology	8.5	1.092
	1	176	20,223	Phosphor technology	10.5	1.107
	1	89	20,056	Phosphor technology	11.5	0.004
	1	88	20,054	Phosphor technology	16.2	0.127
	1	33	09,029	Phosphor technology	19.8	1.766
	1	116	20,131	Phosphor technology	24.1	1.023
	1	99	19,275	Phosphor technology	30.0	0.982
ZnS:Cu	1	28	19,017	Phosphor technology	2.9	0.005
	1	108	14,159	Phosphor technology	9.0	0.056
	1	31	19,018	Phosphor technology	30.0	0.019
ZnS:Mn,Cu	1	96	19,010	Phosphor technology	21.9	1.130
	1	27	19,010	Phosphor technology	22.0	1.519
	1	177	20,267	Phosphor technology		1.585
	1	178	20,268	Phosphor technology		1.337
	1	179	20,269	Phosphor technology		1.038
	1	180	20,270	Phosphor technology		1.496
ZnS:Cu,Pb	1	97	15,027	Phosphor technology	19.0	0.034
ZnS:Cu,Pb,Mn	1	95	17,002	Phosphor technology	19.3	1.017
MgF <sub>2</sub> :Mn	1	138	09,147	Phosphor technology		0.029
La <sub>2</sub> O <sub>2</sub> S:Eu	1	15	10,185	Phosphor technology		0.004
Y <sub>2</sub> O <sub>2</sub> S:Eu	1	90	19,145	Phosphor technology		0.000
EuD <sub>4</sub> TEA	0.1	9	None	Sandia National Laboratories <sup>c</sup>		0.960
	0.1	181	3	Alabama A&M University		2.063
EuD <sub>4</sub> TEA + 1.25 mL DMMP	0.1	194	10	Alabama A&M University		3.196

<sup>a</sup>Ratio based on the TL light yield for both the 1 and 0.1 g samples of 7.5  $\mu\text{m}$  ZnS:Mn (LM-34) set equal to 1.000

<sup>b</sup>The Center for Integrated Nanotechnologies (CINT) is located in Albuquerque, New Mexico

<sup>c</sup>Sandia National Laboratories is located in Livermore, California

point and chemical compatibility of some highly efficient TL materials with Ciba resin systems (MY750/HY956 or MY750/HY917) as illustrated in Table 1.3. A good interface is also needed for effective load transfer to the crystal for adequate TL excitation.

**Table 1.3** Melting points and chemical compatibility of a range of highly triboluminescent materials [54]

Material	Melting point (°C)	Chemical compatibility
Eu complex	170–250	Y
Tb complex	155–290	Y
Mn complex I	230	Y
Mn complex II	300	Y
U complex	60	-
Ester	195	Y
Acetyl complex	185	Y
Aspirin derivative	135	Y

## 1.5 Conclusion

Although extensive work has been done in the synthesis and characterization of triboluminescent materials, there still remains significant gaps in the understanding of the underlying mechanisms responsible for the phenomenon. Work is ongoing to develop triboluminescence-based sensors as load, damage, and impact monitoring systems in engineering systems such as civil and aerospace structure. The key requirements for triboluminescent materials for such applications include large triboluminescent emission yield, be readily available, be environmentally benign, and be compatible with the host material. The ZnS:Mn and EuD<sub>4</sub>TEA are the leading materials for these applications because of their high triboluminescent yields. The ZnS:Mn, because it is inorganic, has however exhibited higher durability property compared to the organic EuD<sub>4</sub>TEA.

## References

1. O'Hara, P. B., Engelson, C., & St Peter, W. (2005). Turning on the light: Lessons from luminescence. *Journal of Chemical Education*, 82, 49–52.
2. Vishwakarma, K., Ramrakhiani, M., & Chandra, B. P. (2007). Luminescence and its application. *International Journal of Nanotechnology and Applications*, 1, 29–34.
3. Olawale, D. O., Dickens, T., Sullivan, W. G., Okoli, O. I., Sobanjo, J. O., & Wang, B. (2011). Progress in triboluminescence-based smart optical sensor system. *Journal of Luminescence*, 131, 1407–1418.
4. Virk, H. S. (2015). History of luminescence from ancient to modern times. *Defect and Diffusion Forum*, 361, 1–13.
5. Goedeke, S., Allison, S., Womack, F., Bergeron, N., Hollerman, W. (2003). Triboluminescence and its application to space-based damage sensors. *Proceedings of the Propulsion Measurement Sensor Development Workshop*. Huntsville, Alabama.
6. Kawaguchi, Y. (1998). Fractoluminescence spectra in crystalline quartz. *Japanese Journal of Applied Physics: Part 1-Regular Papers Short Notes and Review Papers*, 37, 1892–1896.
7. Reynolds, G. T. (1997). Piezoluminescence from a ferroelectric polymer and quartz. *Journal of Luminescence*, 75, 295–299.

8. Chandra, B. P., Elyas, M., & Majumdar, B. (1982). Dislocation models of mechanoluminescence in [gamma]- and X-irradiated alkali halides crystals. *Solid State Communications*, *42*, 753–757.
9. Chandra, B. P., & Shrivastava, K. K. (1978). Dependence of mechanoluminescence in rochelle-salt crystals on the charge-produced during their fracture. *Journal of Physics and Chemistry of Solids*, *39*, 939–940.
10. Nevshupa, R., & Hiratsuka, K. (2015). Triboluminescence. In E. Gnecco & E. Meyer (Eds.), *Fundamentals of friction and wear on the nanoscale*. Cham: Springer International Publishing.
11. Bergeron, N. P., Hollerman, W. A., Goedeke, S. M., Hovater, M., Hubbs, W., Finchum, A., et al. (2006). Experimental evidence of triboluminescence induced by hypervelocity impact. *International Journal of Impact Engineering*, *33*, 91–99.
12. Sweeting, L. M. (2001). Triboluminescence with and without air. *Chemistry of Materials*, *13*, 854–870.
13. Walton, A. J. (1977). Triboluminescence. *Advances in Physics*, *26*, 887–948.
14. Derjaguin, B. V., Krotova, N. A., & Toporov, Y. P. (1981). Emission of high-speed electrons and other phenomena accompanying the process of breaking adhesion bonds. In J. M. Georges (Ed.), *Tribology series*. Amsterdam: Elsevier.
15. Miura, T., Chini, M., & Bennewitz, R. (2007). Forces, charges, and light emission during the rupture of adhesive contacts. *Journal of Applied Physics*, *102*, 103509.
16. Licoppe, C. (2013). La formation de la pratique scientifique: le discours de l'expérience en France et en Angleterre (1630–1820), La découverte.
17. Weiser, H. B. (1918). Crystalloluminescence II. *The Journal of Physical Chemistry*, *22*, 576–595.
18. Brenner, M. P., Hilgenfeldt, S., & Lohse, D. (2002). Single-bubble sonoluminescence. *Reviews of Modern Physics*, *74*, 425.
19. Tsuboi, Y., Seto, T., & Kitamura, N. (2008). Laser-induced shock wave can spark triboluminescence of amorphous sugars. *The Journal of Physical Chemistry. A*, *112*, 6517–6521.
20. Butyagin, P. Y., Yerofeyev, V., Musayelyan, I., Patrikeyev, G., Streletskii, A., & Shulyak, A. (1970). The luminescence accompanying mechanical deformation and rupture of polymers. *Polymer Science U S S R*, *12*, 330–342.
21. Xu, C. N., Watanabe, T., Akiyama, M., & Zheng, X. G. (1999). Direct view of stress distribution in solid by mechanoluminescence. *Applied Physics Letters*, *74*, 2414–2416.
22. Urbakh, M., Klafter, J., Gourdon, D., & Israelachvili, J. (2004). The nonlinear nature of friction. *Nature*, *430*, 525–528.
23. Chandra, B. P. (1998). *Luminescence of solids*. New York: Plenum Press.
24. Chandra, B. P., Baghel, R. N., & Chandra, V. K. (2010). Mechanoluminescent glow curve of ZnS:Mn. *Chalcogenide Letters*, *7*, 1–9.
25. Lu, H.-Y., & Chu, S.-Y. (2004). The mechanism and characteristics of ZnS-based phosphor powders. *Journal of Crystal Growth*, *265*, 476–481.
26. Grmela, L., Macku, R., & Tomanek, P. (2008). Near-field measurement of ZnS:Mn nanocrystal and bulk thin-film electroluminescent devices. *Journal of Microscopy (Oxford)*, *229*, 275–280.
27. Manzoor, K., Vadera, S. R., Kumar, N., & Kutty, T. R. N. (2004). Multicolor electroluminescent devices using doped ZnS nanocrystals. *Applied Physics Letters*, *84*, 284–286.
28. Suyver, J. F., Wuister, S. F., Kelly, J. J., & Meijerink, A. (2001). Synthesis and Photoluminescence of Nanocrystalline ZnS:Mn<sup>2+</sup>. *Nano Letters*, *1*, 429–433.
29. Wood, V., Halpert, J. E., Panzer, M. J., Bawendi, M. G., & Bulovic, V. (2009). Alternating current driven electroluminescence from ZnSe/ZnS:Mn/ZnS nanocrystals. *Nano Letters*, *9*, 2367–2371.
30. Chandra, B. P., Xu, C. N., Yamada, H., & Zheng, X. G. (2010). Luminescence induced by elastic deformation of ZnS:Mn nanoparticles. *Journal of Luminescence*, *130*, 442–450.

31. Kobayakov, I. B., & Pado, G. S. (1968). Investigation of electrical and elastic properties of hexagonal zinc sulfide in temperature range 1.5-300 degrees K. *Soviet Physics Solid State*, 9, 1707.
32. Chandra, B. P., & Rathore, A. S. (1995). Classification of mechanoluminescence. *Crystal Research and Technology*, 30, 885–896.
33. Sage, I., & Bourhill, G. (2001). Triboluminescent materials for structural damage monitoring. *Journal of Materials Chemistry*, 11, 231–245.
34. Chudacek, I. (1966). Influence of pressure on recombination centres in piezoelectric luminophores. *Czechoslovak Journal of Physics*, 16, 520–524.
35. Chudacek, I. (1967). Kinetics of triboluminescence of zinc sulphide I. *Czechoslovak Journal of Physics*, 17, 34–42.
36. Chandra, B. P., Bagri, A. K., & Chandra, V. K. (2010). Mechanoluminescence response to the plastic flow of coloured alkali halide crystals. *Journal of Luminescence*, 130, 309–314.
37. Allison, S. W., & Gillies, G. T. (1997). Remote thermometry with thermographic phosphors instrumentation and applications. *The Review of Scientific Instruments*, 68, 2615–2650.
38. Chandra, B. P., Baghel, R. N., Singh, P. K., & Luka, A. K. (2009). Deformation-induced excitation of the luminescence centres in coloured alkali halide crystals. *Radiation Effects and Defects in Solids*, 164, 500–507.
39. Chandra, B. P., Singh, S., Ojha, B., & Shrivastava, R. G. (1996). Mobile interstitial model and mobile electron model of mechano-induced luminescence in coloured alkali halide crystals. *Pramana: Journal of Physics*, 46, 127–143.
40. Molotskii, M. I., Poletaev, A. V., & Shmurak, S. Z. (1989). Dislocation-induced sensibilization of photoelectronic emission. *Fizika Tverdogo Tela*, 31, 14–20.
41. Chakravarty, A., & Phillipson, T. E. (2004). Triboluminescence and the potential of fracture surfaces. *Journal of Physics D: Applied Physics*, 37, 2175–2180.
42. Destriau, G. (1936). Recherches sur les scintillations des sulfures de zinc aux rayons@, R. Bussière.
43. Shionoya, S., Yen, W. M., & Hase, T. (1999). *Phosphor handbook*. Boca Raton, FL: CRC Press.
44. Hurt, C. R., Mcavoy, N., Bjorklund, S., & Filipescu, N. (1966). High intensity triboluminescence in europium tetrakis (dibenzoylmethide)-triethylammonium. *Nature*, 212, 179–180.
45. Hollerman, W. A., Fontenot, R. S., Bhat, K. N., Aggarwal, M. D., Guidry, C. J., & Nguyen, K. M. (2012). Comparison of triboluminescent emission yields for 27 luminescent materials. *Optical Materials*, 34, 1517–1521.
46. Olawale, D. O., Dickens, T., Lim, A., Okoli, O., Wang, B., & Sobanjo, J. O. (2010). *Characterization of the triboluminescence (TL) performance of ZnS:Mn under repeated mechanical loading for smart optical damage sensor system. NDE/NDT for highways and bridges: Structural materials and technology (SMT) 2010*. New York, USA: American Society of Non-Destructive Testing (ASNT).
47. Sage, I., Humberstone, L., Oswald, I., Lloyd, P., & Bourhill, G. (2001). Getting light through black composites: Embedded triboluminescent structural damage sensors. *Smart Materials and Structures*, 10, 332–337.
48. Womack, F. N., Goedeke, S. M., Bergeron, N. P., Hollerman, W. A., & Allison, S. W. (2004). Measurement of triboluminescence and proton half brightness dose for ZnS:Mn. *IEEE Transactions on Nuclear Science*, 51, 1737–1741.
49. Xu, C. N., Watanabe, T., Akiyama, M., & Zheng, X. G. (1999). Preparation and characteristics of highly triboluminescent ZnS film. *Materials Research Bulletin*, 34, 1491–1500.
50. Chandra, B. P., & Zink, J. I. (1980). Triboluminescence and the dynamics of crystal fracture. *Physical Review B*, 21, 816–826.
51. Kim, J. S., Kwon, Y. N., Shin, N., & Sohn, K. S. (2007). Mechanoluminescent SrAl<sub>2</sub>O<sub>4</sub>: Eu, Dy phosphor for use in visualization of quasidynamic crack propagation. *Applied Physics Letters*, 90, 241916.

52. Sohn, K. S., Seo, S. Y., Kwon, Y. N., & Park, H. D. (2002). Direct observation of crack tip stress field using the mechanoluminescence of SrAl<sub>2</sub>O<sub>4</sub>:(Eu, Dy, Nd). *Journal of the American Ceramic Society*, 85, 712–714.
53. Xu, C. N., Zheng, X. G., Akiyama, M., Nonaka, K., & Watanabe, T. (2000). Dynamic visualization of stress distribution by mechanoluminescence image. *Applied Physics Letters*, 76, 179–181.
54. Sage, I., Badcock, R., Humberstone, L., Geddes, N., Kemp, M., & Bourhill, G. (1999). Triboluminescent damage sensors. *Smart Materials and Structures*, 8, 504–510.

# Chapter 2

## Nature of the Electronic Charge Carriers Involved in Triboluminescence

Friedemann T. Freund

### 2.1 Introduction

Luminescence describes the emission of light from matter, mostly solids, that is not generated by heat. Different actions can cause luminescence. Triboluminescence, for instance, is caused by mechanical action. Some major questions arise: How does mechanical action produce luminescence and why can it be observed in some materials but not in others?

When solids are subjected to compressive or tensile forces, they deform. At first, within the elastic range, deformation is proportional to the applied force. At higher stresses deformation becomes non-linear. Eventually the solids will fracture creating new surfaces.

Microscopically, fracturing means that interatomic bonds are broken as a fracture propagates through the solid medium creating two opposite surfaces, which begin to separate. Because of the stochastic nature of any fracture event these fracture surfaces will contain atoms/ions with dangling bonds and will carry patches of charges of opposite signs. As the surfaces separate, electric ( $E$ ) fields develop, which can be high to very high. These  $E$  fields momentarily accelerate electrons and ions emitted from the fracture surfaces. The  $E$  fields are particularly high at the tip of propagating cracks—high enough to accelerate electrons and ions over short distances to such high energies that they impact-ionize gas neutrals, creating additional electrons and ions, and causing avalanche electric discharges. Such discharges produce bursts of light with spectra extending through the visible (VIS) into the ultraviolet (UV) and even into the X-ray region [1]. The high-energy portion of this light will surely interact with the bulk of the solid and initiate secondary reactions.

---

F.T. Freund (✉)

GeoCosmo Science Center – NASA Ames Research Park, Bldg 19,  
Suite 1070-I, Moffett Field 94035, CA, USA  
e-mail: [friedemann.t.freund@nasa.gov](mailto:friedemann.t.freund@nasa.gov)

Interesting from the viewpoint of triboluminescence are cases when the emitted light is colored and does not only come from the narrow gap between the fracture surfaces or from the fracture surfaces themselves, but from the inside of the bulk. Often triboluminescence is produced by relatively gentle mechanical actions such as rubbing or tumbling. Though rubbing or tumbling may cause spallation and microfractures on very small scales, they are a far cry from the highly energetic processes that take place during macroscopic fracture. If there is persistent light emission coming from within the bulk during rubbing or tumbling, we have to consider mechanisms, by which relatively large bunches of energy are created with very small input of mechanical energy, flowing from the surface or near-surface region, where the mechanical action had taken place, into the underlying bulk.

This chapter deals primarily with oxide materials. It reports on a specific type of point defects in oxide materials that has been consistently overlooked by the scientific community: peroxy defects, where oxygen changes its valence from 2– to 1–. Peroxy defects occur in many oxides and in silicates. They occur in rocks. It will be argued here that peroxy defects and the highly mobile positive hole charge carriers, which they engender, play a major role in energy transfer processes that allow triboluminescence to occur at sites, which are some distance away from the sites of the mechanical action. At the end of this chapter the insight gained from studying peroxy defects and positive holes in oxide materials will be extended to non-oxide materials.

## 2.2 Peroxy—The Stealth Defects

### 2.2.1 Band Structure and Electronic Charge Carriers

Any form of luminescence requires the formation of excited states, commonly electronically excited states, and their de-excitation via radiative transitions. If the light emission falls into the visible (VIS) range, their photon energies range from 1.65 eV in the red (750 nm) to 3.1 eV in the violet (400 nm). Since  $kT$ , the mean thermal energy<sup>1</sup> at 300 K, is only 25 meV, the energy emitted over this spectral region is 25–65 times the amount of energy available through  $kT$ . Two questions thus arise: (1) where does the energy come from that can lead to the emission of photons in the VIS region and (2) how does this energy travel through the solid medium from the site of mechanical action to the site of photon emission.

To start it may be good to look at some fundamental issues regarding electronic charge carriers in solids. Figure 2.1a and b sketches the valence and conduction bands for semiconductors and insulators, respectively. The difference between the two classes of materials lies in the width of the bandgap  $E_g$ . In a semiconductor  $E_g$  is sufficiently narrow for some electrons from the fully occupied valence band to be

---

<sup>1</sup> With  $k$  being the Boltzmann constant and  $T$  the absolute temperature.

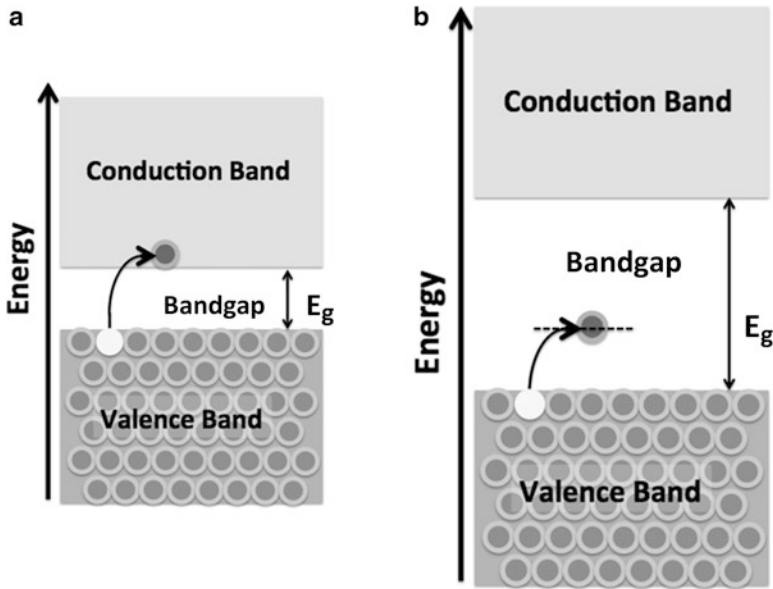


**Fig. 2.1** (a, b) Schematic representation of the band structure of (a) a semiconductor and (b) an insulator, both with fully occupied valence bands.  $E_g$  is the width of the band gap. The arrows indicate that electrons can be thermally activated (by  $kT$ ) into the conduction band or into impurity levels in the band gap, respectively. Figure b indicates that, when  $E_g$  is much wider than the thermal energy  $kT$  as is the case in insulators, electrons cannot be thermally activated to the conduction band. However, if impurities create energy levels in the band gap that can act as acceptors, electrons from the valence band can be promoted to these impurity levels. Unless their density is so high that their wave functions partly overlap, electrons on those impurity levels will be localized and do not contribute to the electrical conductivity

thermally promoted into the conduction band due to the thermal energy  $kT$ , where  $k$  is the Boltzmann constant and  $T$  the absolute temperature. The promotion of an electron into the conduction band leaves a defect electron in the valence band, also known as a hole [2]. In the intrinsic case the ratio of the number of electrons in the conduction band  $n'$  and the number of holes in the valence band  $n^*$  is 1. Electrons and holes are both mobile, albeit with different mobilities,  $\mu'$  and  $\mu^*$ , respectively, with electrons being typically more mobile than holes.

### 2.2.2 Peroxy Defects in Oxide Materials, Minerals, and Rocks

The  $O^{2-}$  anions in oxide materials are commonly assumed to be in the 2- valence state and in the 2- valence state only. However, oxygen can exist in two valence states, 1- and 2-. A peroxy defect consists of two oxygen anions oxidized from

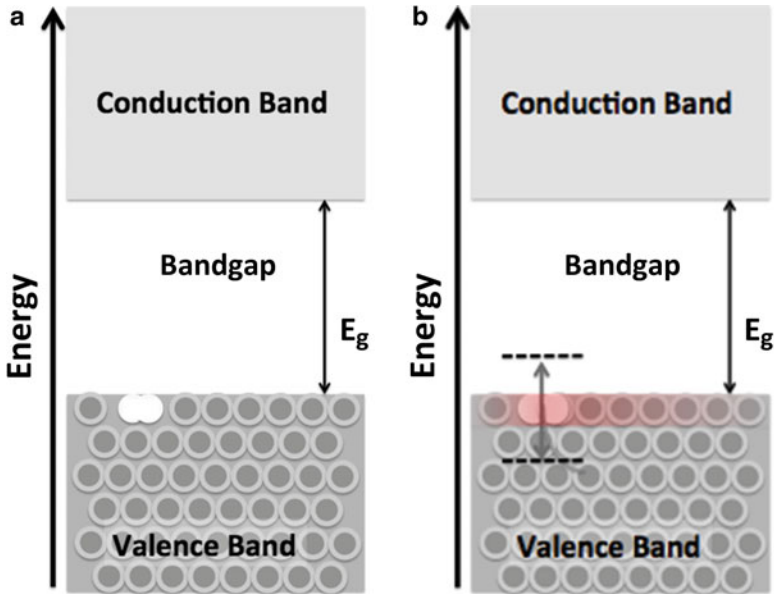


**Fig. 2.2** (a) Schematic representation of the effect of a peroxy defect on the energy surface of the valence band of an oxide insulator. The majority  $2-$  oxygen anions are shown in *dark gray*. The white dumbbell represents a dip in the energy surface of the valence band due to the presence of a peroxy defect. (b) When a peroxy defect becomes activated, it generates two states: an electron that remains trapped in the broken peroxy bond and a hole that delocalizes over many neighboring  $O^{2-}$  and becomes as mobile charge carrier

$2-$  to  $1-$ . Figure 2.2a and b sketches a situation, where a peroxy defect is introduced into an oxide material. It is equivalent to two holes trapped on two adjacent  $O^{2-}$  sites. Since the  $-1$  valence state primarily affects energy levels of O  $2sp$  symmetry at the upper edge of the valence band, peroxy defects manifest themselves by a local dip in the energy surface of the valence band as indicated in Fig. 2.2a.

When the  $O^-O^-$  bond breaks, an electron can be transferred into the broken peroxy bond from an outside  $O^{2-}$ . This electron gets trapped in the broken peroxy bond, occupying an energy level slightly below the edge of the valence band as indicated by lower dashed line in Fig. 2.2b. By symmetry an empty energy level is created slightly above the edge of the valence band, as indicated by the upper dashed line in Fig. 2.2b. The donor  $O^{2-}$  turns into an  $O^-$ , i.e., into a defect electron in the  $O^{2-}$  sublattice, e.g., a hole. As will be argued further below this hole state tends to delocalize over many  $O^{2-}$  neighbors as indicated by the reddish hue in Fig. 2.2b. Because of this and of other rather remarkable properties associated with this hole state in the oxygen anion sublattice, it has been given the name “positive hole” [3].

Much of what follows from here onward derives from the noteworthy properties of positive holes, which the peroxy defects release when they break up. A major point will be to examine how peroxy defects and positive holes contribute to luminescence phenomena and specifically to triboluminescence.

### 2.2.3 *Nature of Electronic Charge Carriers, Electrons, and Holes, in Insulating Oxide Materials*

Peroxy defects are a family of point defects in oxide materials that have not received the attention they probably deserve. Though they seem to be ubiquitous across a wide range of oxide materials and rock-forming minerals, their presence has been largely overlooked.

Peroxy defects consist of pairs of oxygen anions, which have changed their valence from the usual  $2-$  state to  $1-$ , where  $O^-$  is more oxidized than  $O^{2-}$ . The two  $O^-$  are covalently bonded, forming a very short  $O^-O^-$  bond, only  $\sim 1.5 \text{ \AA}$  as compared to the usual  $2.8\text{--}3.0 \text{ \AA}$  distances between adjacent  $O^{2-}$ . Though the activation energy to dissociate peroxy bonds is relatively high, on the order of  $2.4 \text{ eV}$  in MgO [4] and probably similar in other oxide matrices, they are also quite labile. They break up, when an electron is transferred from some nearby  $O^{2-}$  into the peroxy bond and becomes trapped, leaving one  $O^-$  with the broken peroxy bond. This  $O^-$  is stationary, while the donor  $O^{2-}$  turns into  $O^-$  and becomes a mobile positive hole charge carrier, which can move away from its point of origin. There is strong evidence that the wave function associated with this mobile  $O^-$  state, e.g. with the positive hole, is highly delocalized over the O  $2sp$ -type energy levels that form the upper edge of the valence band [5, 6]. The peroxy dissociation can of course reverse by the mobile hole recombining with another mobile hole or with a defect-bound  $O^-$ .

$O^-$  have a strong propensity to take over an electron to return to the  $O^{2-}$  state. Thus they act as oxidizing agents. When positive holes roam through the bulk, they can interact with transition metal cations and participate in charge transfer processes. This is the reason why positive holes are interesting actors in the context of luminescence, including triboluminescence.

Since peroxy defects and positive holes have not been widely discussed in the literature yet—except in papers by the present author—the work presented here and the references quoted will primarily tap this source of information. Magnesium oxide, MgO, played a major role in the discovery of peroxy defects and positive holes. Subsequently peroxy defects and positive hole-type charge carriers have been shown to also exist in other oxide materials, including silicates. There is evidence that similar defects also exist in non-oxide materials.

## 2.3 Discovery and Validation of Peroxy Defects

### 2.3.1 *Formation of Oxygen Anions in the $1-$ Valence State*

Peroxy defects were first observed in MgO, the structurally simplest oxide, face-centered cubic. As a main group element Mg has only one chemically stable